ARL-TN-1086 ● SEP 2021

DEVCOM ARMY RESEARCH LABORATORY

Polarimetric Longwave Infrared (LWIR) Thermal Vision for Autonomous Vehicle Operation

by Kristan P Gurton

NOTICES

Disclaimers

The findings in this report are not to be construed as an official Department of the Army position unless so designated by other authorized documents.

Citation of manufacturer's or trade names does not constitute an official endorsement or approval of the use thereof.

Destroy this report when it is no longer needed. Do not return it to the originator.

ARL-TN-1086 ● SEP 2021

Polarimetric Longwave Infrared (LWIR) Thermal Vision for Autonomous Vehicle Operation

Kristan P Gurton
Computational and Information Sciences Directorate,
DEVCOM Army Research Laboratory

REPORT DOCUMENTATION PAGE

Form Approved
OMB No. 0704-0188

1. REPORT DATE *(DD-MM-YYYY)*	2. REPORT TYPE	3. DATES COVERED (From - To)
September 2021	Technical Note	January–August 2021

4. TITLE AND SUBTITLE
Polarimetric Longwave Infrared (LWIR) Thermal Vision for Autonomous Vehicle Operation

5a. CONTRACT NUMBER

5b. GRANT NUMBER

5c. PROGRAM ELEMENT NUMBER

6. AUTHOR(S)
Kristan P Gurton

5d. PROJECT NUMBER

5e. TASK NUMBER

5f. WORK UNIT NUMBER

7. PERFORMING ORGANIZATION NAME(S) AND ADDRESS(ES)
DEVCOM Army Research Laboratory
ATTN: FCDD-RLC-ES
Adelphi, MD 20783-1138

8. PERFORMING ORGANIZATION REPORT NUMBER
ARL-TN-1086

9. SPONSORING/MONITORING AGENCY NAME(S) AND ADDRESS(ES)

10. SPONSOR/MONITOR'S ACRONYM(S)

11. SPONSOR/MONITOR'S REPORT NUMBER(S)

12. DISTRIBUTION/AVAILABILITY STATEMENT
Approved for public release: distribution unlimited.

13. SUPPLEMENTARY NOTES

14. ABSTRACT
This report describes results of a field study conducted to assess the utility of using polarization-augmented thermal vision to enhance autonomous vehicle operation. In particular, polarimetric and conventional long-wave infrared (LWIR) video was recorded for a variety of nighttime driving scenarios conducted in both rural and urban environments. An uncooled microbolometer-based LWIR polarimetric camera sensor capable of recording simultaneous conventional thermal and polarimetric video imagery was used. Results showed improved spatial detail and information content for polarization-augmented thermal imagery when compared to conventional thermal only.

15. SUBJECT TERMS
polarimetric imaging, thermal vision, autonomous, machine learning, ML, artificial intelligence, AI

16. SECURITY CLASSIFICATION OF:			17. LIMITATION OF ABSTRACT	18. NUMBER OF PAGES	19a. NAME OF RESPONSIBLE PERSON
a. REPORT	b. ABSTRACT	c. THIS PAGE			Kristan P Gurton
Unclassified	Unclassified	Unclassified	UU	20	19b. TELEPHONE NUMBER (Include area code) (301) 394-2093

Contents

List of Figures

List of Tables

1. Introduction

The science and technologies associated with autonomous vehicle operation are rapidly evolving and changing in order to ever increase safety and reliability. Early forms of semiautonomous vehicle operation often used one or more conventional ranging technologies based on the reflection of light, sound, or radio waves (i.e., light-detection-and-ranging [LIDAR], sound-navigation-and-ranging [SONAR], and radio-detection-and-ranging [RADAR]).[1] Recent efforts by commercial manufactures to produce fully autonomous vehicles have incorporated various forms of artificial intelligence (AI) and machine learning (ML) algorithms that rely on multiple sets of visible-based video cameras.[2] In an effort to improve video performance for nighttime and/or extreme weather conditions, visible cameras are often actively illuminated with near-IR beacons, but are limited in range to about 8–12 m.[3] These visible-based video systems appear to perform adequately for driving conditions that are well to moderately illuminated, but are less effective under conditions of poor illumination (e.g., extreme rain, fog, snow, and so on). Under such conditions, the use of cost-effective thermal IR vision may be warranted. This option has become commercially viable with costs for uncooled microbolometer focal-plane arrays (FPAs) well under $1000.[4] In addition, the Army (as well as other DOD agencies) are actively pursuing new methods and technologies for autonomous vehicle operation on the battlefield in which no form of active illumination is required (i.e., stealth operation).[5] Although thermal vision, either in the longwave-infrared (LWIR) or midwave-infrared (MidIR) spectral bands, has the ability to operate in complete darkness, the resultant imagery often lacks the spatial detail often seen in conventional visible-based imagery.

To improve the spatial resolution in both MidIR and LWIR thermal imagery, the Army is developing new technologies designed to exploit the polarization-state information that is inherent in all image-forming radiance (i.e., thermal polarimetric imaging).[6–10] A polarimetric image is a 2-D representation of a given scene in which the intensity of each pixel represents the magnitude of linear polarization of the image-forming emission. Because polarization state information is highly dependent on surface geometry, a polarimetric image exhibits additional spatial information that is often lost in a temperature-based thermal image. An example showing improved spatial content for a LWIR polarimetric image compared to a conventional LWIR thermal image is shown in Fig. 1.

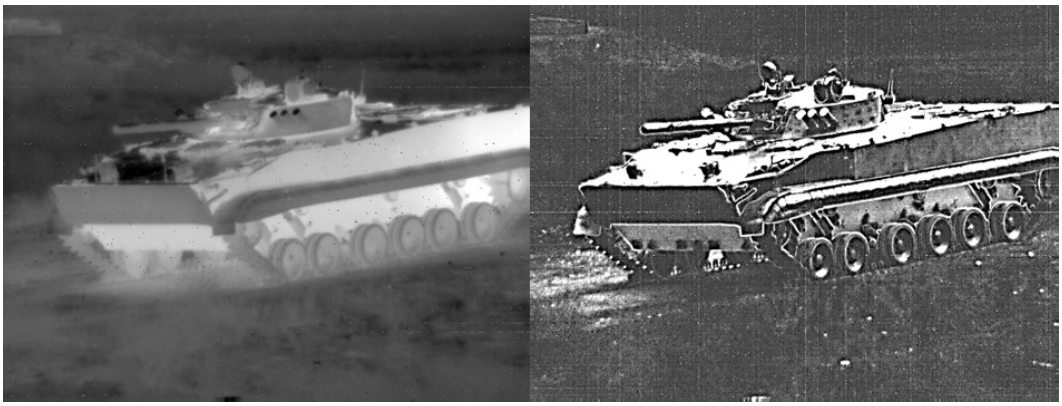

Fig. 1 LWIR thermal (left) and the resultant polarimetric degree-of-linear-polarization (DoLP) image (right) comparison of a Russian 1970s vintage T-72 tank

For polarimetric applications, it is common practice to use a Stokes parameter approach to describe the polarization state of the image-forming radiation that results from either emission or reflection.[11] We apply the Stokes parameter methodology to our imaging application where the Stokes parameters images S1, S2, and S0 are defined by Eqs. 1–3:

$$S1 = I(0) - I(90) \quad (\text{w/sr-m}^2), \tag{1}$$

$$S2 = I(+45) - I(-45) \quad (\text{w/sr-m}^2), \tag{2}$$

$$S0 = \text{total calibrated radiance image} \quad (\text{w/sr-m}^2), \tag{3}$$

and the DoLP parameter is defined as

$$\text{DOLP} = \frac{\sqrt{S1^2 + S2^2}}{S0}, \tag{4}$$

where I(0), I(90), I(+45), and I(–45) represent 2-D LWIR images produced with polarimetrically filtered radiance that is polarized (relative to the vertical plane) at 0°, 90°, +45°, or –45°, respectively. As one can see from Eqs. 1–3, the S1 image represents the difference between the vertical and horizontal states, the S2 image represents a measure of the difference between the two ±45° diagonal states, and the combined radiance image, S0, is taken to be the conventional LWIR thermal image. Finally, it is common practice to normalize S1 and S2 with respect to S0 in order to generate a unitless fraction (i.e., S1(%) = 100 × (S1/S0) and S2(%) = 100 × (S2/S0)).

The LWIR polarimetric sensor used is based on an uncooled microbolometer FPA in which micro-grid polarizers oriented at 0°, 90°, 45°, or 135° are affixed to each pixel in a 2 × 2 array format. The microbolometer has a 17-μm pixel pitch with

640 × 512 format. The microbolometer polarimetric camera (called Pyxis) is produced by Polaris Sensor Technologies, Inc. (Huntsville, Alabama), under an Army Small Business Innovation Research contract. Figure 2 shows a schematic of the micro-grid polarizer orientation geometry (left) and a photograph of the LWIR microbolometer-based polarimetric sensor (right). Listed in Table 1 are the technical parameters for the thermal polarimetric camera. A more-detailed description of the polarimetric camera system and methodology used can be found in Chenault et al.[12]

Fig. 2 Schematic of the micro-grid polarizer orientation geometry (left) and a photograph of the LWIR microbolometer-based polarimetric sensor (right) used in this study

Table 1 Technical parameters for the Pyxis microbolometer-based polarimetric camera system produced by Polaris Sensor Technology

Detector	Uncooled VOx microbolometer array
Waveband	7.5–13 um
Pixel pitch	17 mm
Format	640 × 512 pixels
Frame rate	30 Hz
Full-frame pixel operability	>99.9%
NEDT at f/0.87	<50 mK
NEDoLP	<0.5%
Size (without lens)	1.79 × 1.75 × 1.79 inches
Weight without lens	83 g
Input voltage	5 V
Steady-state power at 23 °C	4 W
Peak power at 23 °C	5.3
Data interface	NTSC, 14-bit camera link, GigE

2. Field Test

During the field test, the LWIR polarimetric camera was mounted atop a small sport utility vehicle (SUV) and driven during the late evening hours along a variety of rural and urban roadways. Illumination while driving varied from well-lit

conditions to roadways in which no there was no illumination at all. Road types encountered included smooth and rough asphalt, dirt, gravel, and grass.

Shown next is a series of representative images of various rural scenes recorded while driving during the evening hours from approximately 1 to 3 a.m. The images are single frames taken from the video feed recorded by the polarimetric camera that includes a conventional LWIR thermal image, S0, and one or more corresponding polarimetric images. In certain circumstances, a false-color palette is applied in order to convey additional polarimetric information.[13]

Figure 3 shows the first example of anomaly detection that is inherent to polarimetric imaging. Shown in the figure are all four recorded images, S0, S1, S2, and DoLP, as well as a false-color image in which the color represents a particular Stokes vector as defined in Eqs. 1–2. The scene shows driving along a rural road in which no external lighting was present except that of the headlights of the vehicle. The S0 image represents the conventional LWIR thermal image in which no polarization information is present. The S1 and S2 image represent the difference in intensity of linear polarization state in the horizontal and vertical planes (i.e., S1, and the difference in intensity in the ±45° planes, S2), and the DoLP image represents a superposition of both S1 and S2 information. As one can see, the S2 image appears washed out and devoid of any spatial detail, which signifies that there is very little difference between the polarization states in the ±45° planes. However, the S1 image shows the asphalt road and border region to be polarized in the S1 direction, while the wooded region exhibits no linear polarization "except" for a small region located on the left side of S1 image. This region becomes more apparent in the DoLP image and is represented as a "green" patch in the S0 plus S1 image, which signifies that the hidden object exhibits thermal emission that is linearly polarized in the horizontal plane. This anomaly was identified during the test; we were able to stop and investigate, and determined that the object was an abandoned vehicle that was left in a densely wooded area along the road.

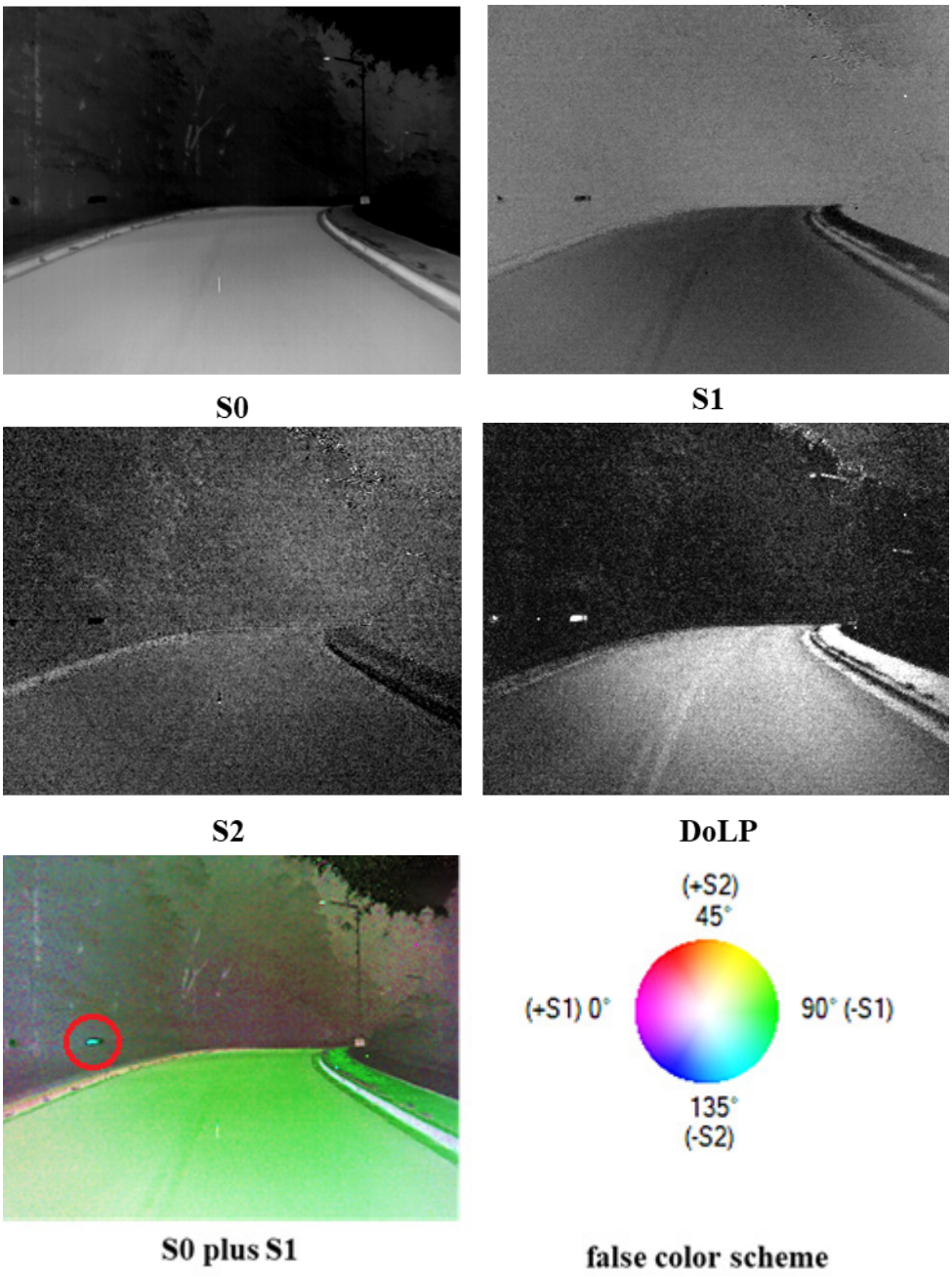

Fig. 3 (Left to right, top to bottom) S0 (conventional LWIR thermal), S1, S2, DoLP, S0 plus S1 information colored in green, and the color palette used to define which Stokes vector is dominate and the direction of polarization as defined in Eq. 1–2

Figure 4 highlights the ability of polarimetric imaging to detect surface defects that are not readily apparent in a conventional thermal image. Shown in Fig. 4 (top left) is the conventional LWIR thermal image, S0, of a rural road in which the asphalt on the right shoulder of the road is worn and deteriorated. As one can see in Fig. 4, the damaged region of the road is clearly visible in both the S1 and DoLP image.

Note the S2 image is not shown since none of the scene exhibited any useful S2 information.

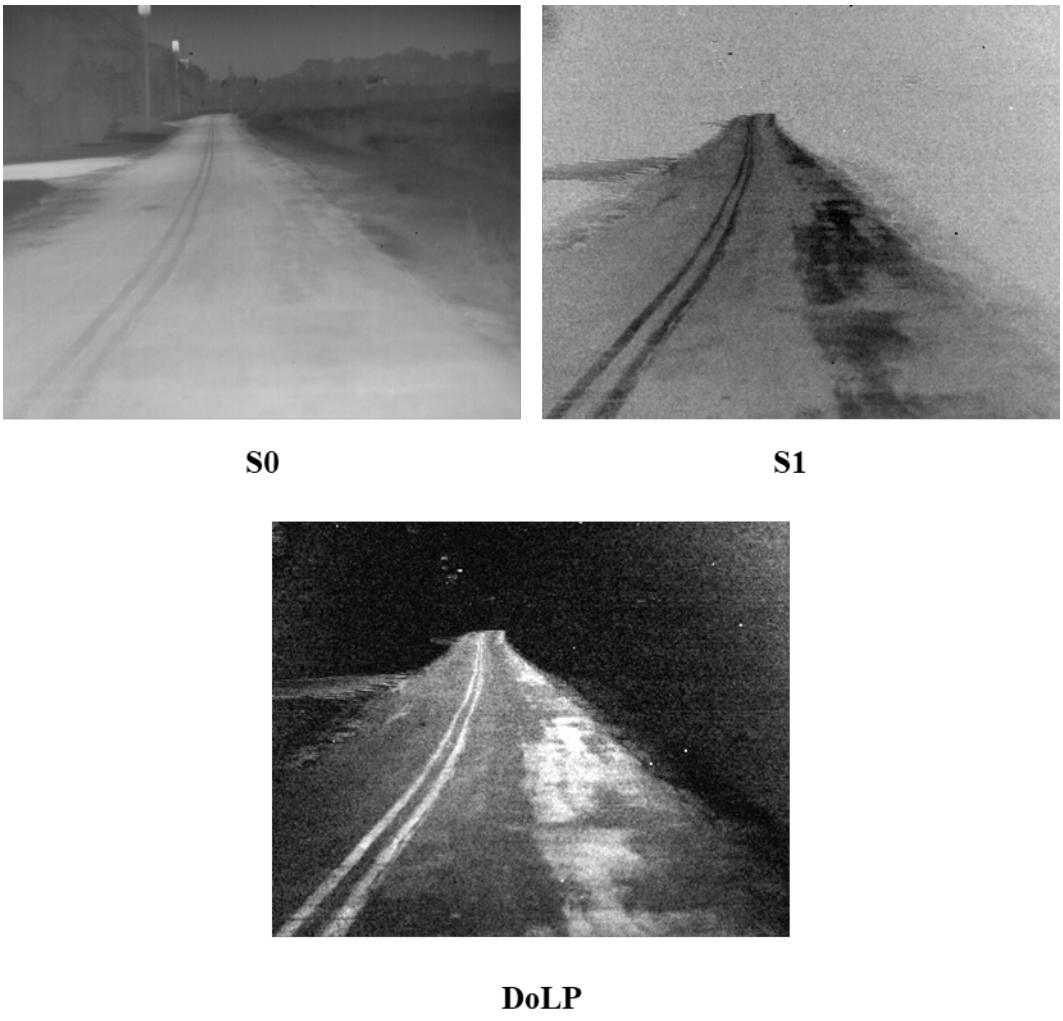

Fig. 4 Image of a rural road in which the road surface is partially damaged. (Top left) The conventional LWIR thermal image, S0, in which the damaged asphalt located on the right shoulder is difficult to discern. However, the S1 and DoLP images (top right and bottom) clearly show the road anomaly.

Figure 5 shows a thermal and polarimetric image set that was recorded at night on a maintenance path used for servicing high-power electrical lines, which consisted of overgrown grass that was approximately 8–10 inches high. During daylight hours, this path was barely visible to the naked eye due to a lack of usage, and during evening hours, it was completely undetectable. Figure 5 (top left) shows the conventional LWIR thermal image, S0, alongside the corresponding polarimetric images S1 and DoLP images (top right and bottom respectively).

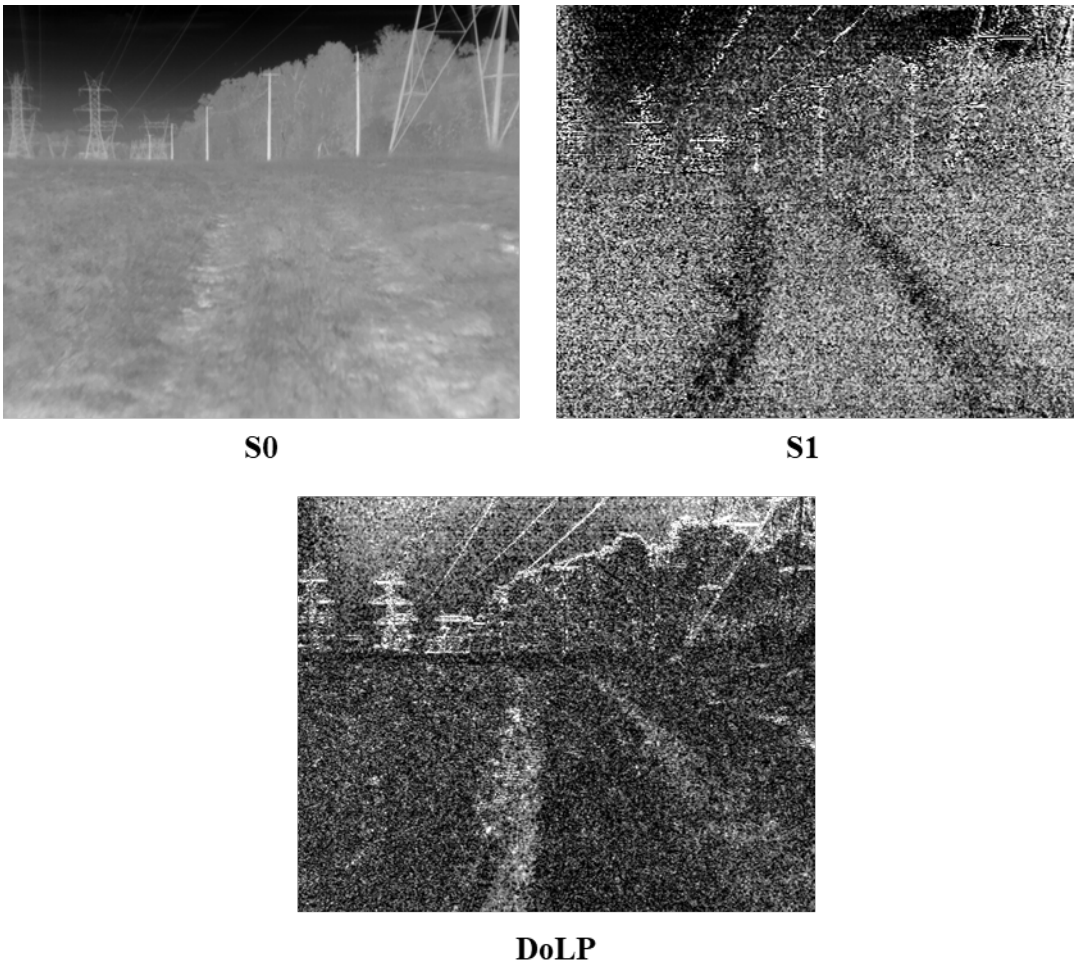

Fig. 5 Thermal and polarimetric image set of a maintenance path used for servicing high-power electrical lines, which consisted of overgrown grass approximately 8–10 inches high

Again it is difficult to identify any clear path via the S0 image, while the S1 and DoLP images show regions of flattened grass tracks that produced measureable changes in the linearly polarized emission of the terrain.

Figure 6 shows an image set of an urban intersection in which an SUV is crossing at a traffic light. Due to a lack of thermal contrast in the LWIR between the SUV and its associated background, it is difficult to see the crossing vehicle in the thermal image S0. However, the polarimetric contrast between the vehicle and background appears good and, as a result, the SUV is displayed more prominently in both the S1 and DoLP images.

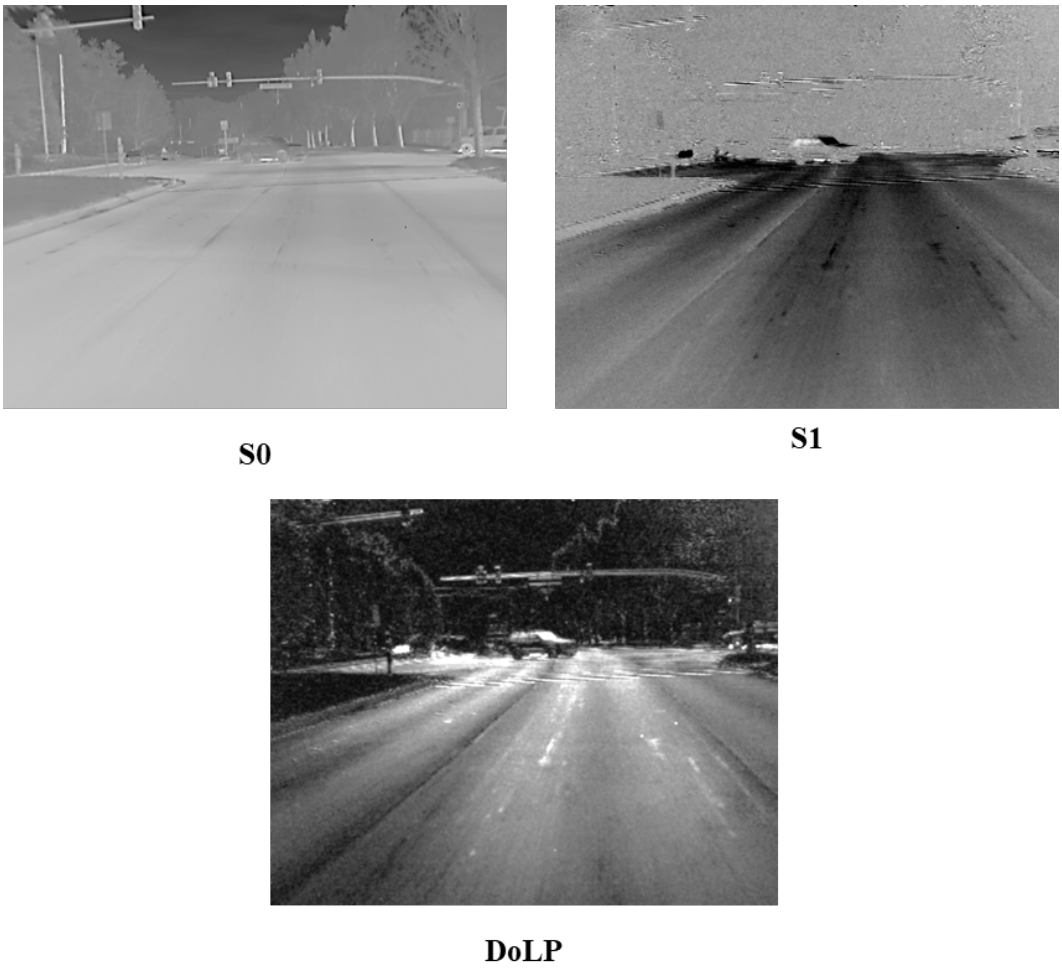

Fig. 6 Thermal and polarimetric image set showing an SUV turning across an intersection

Figure 7 shows a pedestrian crossing at an intersection in which the thermal contrast between the human and the asphalt road is poor (see S0, top left). This lack of contrast is partially attributed to being imaged at night at which time the human's and the asphalt's surface temperatures appear similar. However, since polarimetric contrast does not rely on thermal differences, the contrast in both the S1 and DoLP appears superior compared to the S0 image, and is best highlighted in the color-fused S0-plus-S1 image shown in the bottom right.

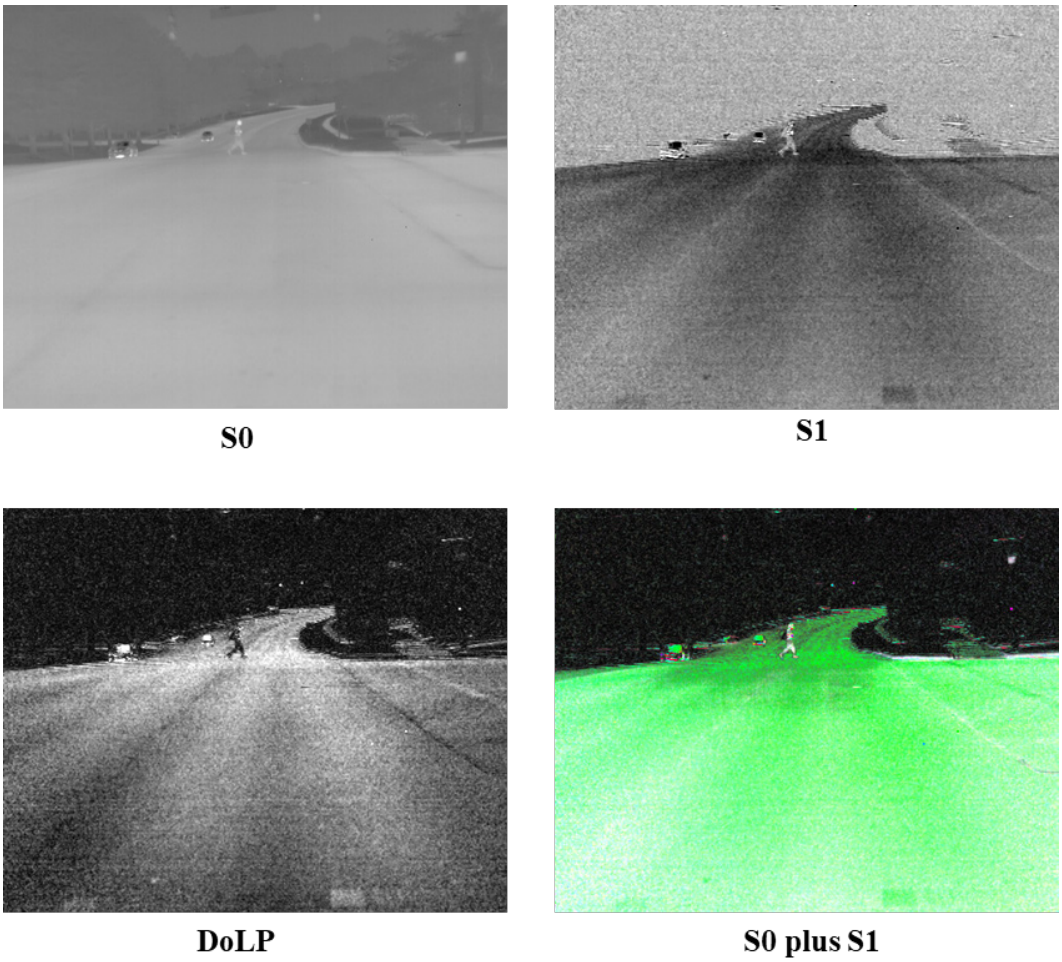

Fig. 7 A pedestrian crossing an asphalt road at night. The ability to identify the human in the thermal S0 image appears difficult due to poor thermal contrast, while the polarimetric images S1 and DoLP display better contrast.

3. Concluding Remarks

We conducted a field test in which thermal and polarimetric video was recorded to assess the applicability for using such imagery to enhance autonomous vehicle operation. The image sets were recorded in the LWIR portion of the spectrum using a novel thermal polarimetric camera system that utilizes an uncooled microbolometer FPA. Operation was conducted during nighttime conditions for both urban and rural driving scenarios.

Results showed under certain conditions that thermal contrast in the LWIR between obstacles and the associated background was less than desirable, as shown in Figs. 6 and 7, and that this condition could be greatly improved by augmenting the conventional thermal image with polarimetric information. Figures 3, 4, and 5 show

examples of improved detection of hidden objects and subtle surface anomalies in the thermal IR when polarimetric imaging is applied.

In future, both civilian and military autonomous vehicle operation will be heavily dependent on vision centric-based systems that only require efficient and reliable AI algorithms for navigation.[14] The ability of a ML or AI algorithm to rapidly converge on a solution (e.g., whether to apply the brakes) is highly dependent on nature of the image set that is being processed. Ideally, such systems would operate more efficiently when processing image sets that are devoid of unnecessary clutter and information that is not relevant for safe navigation. A polarimetric filtered image set may offer such a solution (Fig. 8).

Fig. 8 Comparison of image information content appropriate for AI or ML autonomous vehicle operation: a conventional LWIR thermal image S0 (left) and the resultant "simplified" S1 polarimetric image (right)

As one can see, the polarimetric image, S1 (right) produces a simplified scene by suppressing much of the natural environment, thus leaving only the oncoming vehicles and the profile of the road. However, it is not clear whether such a simplified image set would produce better performance for autonomous navigation and further testing is warranted.

Finally, although this data set was limited, efforts are underway to expand the scope of this work to include test scenarios that are more appropriate for DOD applications.

4. References

1. Au T, Zhang S, Stone P. Autonomous intersection management for semi-autonomous vehicles. Routledge Handbook of Transportation, Routledge Press; 2005.

2. Janai J, Guney F, Behl A. Computer vision for autonomous vehicles: problems, datasets and state of the art. Foundations and Trends in Computer Graphics and Vision. 2020;12(1–3):1–308.

3. Kane M. See what Tesla autopilot sees at night in rain: video. Insideevs; 2019 May 7. https://insideevs.com/news/348362/video-what-tesla-autopilot-sees-night-rain/.

4. Yu L, Guo Y, Zhu H, Luo M, Han P, Ji X. Low-cost microbolometer type infrared detectors. J Micromachines. 2020;11(9):800.

5. US DARPA selects research teams for invisible headlights programme. Army Technology; 2021 July 13. https://www.army-technology.com/news/us-darpa-research-teams-invisible-headlights-programme/.

6. Gurton KP, Edmondson R. MidIR and LWIR thermal polarimetric imaging comparison using reviver operating characteristic (ROC) curve analysis. DEVCOM Army Research Laboratory (US); 2020 Oct. Report No.: ARL-TR-9092.

7. Gurton KP. Calibrated long-wave infrared (LWIR) thermal and polarimetric imagery of small unmanned aerial vehicles (UAVs) and birds. Army Research Laboratory (US); 2018 Aug. Report No.: ARL-TR-8475.

8. Gurton KP, Yuffa A, Videen G. Enhanced facial recognition for thermal imagery using polarimetric imaging. Opt Lett. 2014;39(13):3857–3859.

9. Felton M, Gurton K, Pezzaniti L. Measured comparison of the crossover periods for mid- and long-wave IR (MWIR and LWIR) polarimetric and conventional thermal imagery. Optics Express. 2010;18(15):15704–15713.

10. Gurton KP, Felton M, Pezzaniti L. Remote detection of buried land-mines and IEDs using LWIR polarimetric imaging. Optics Express. 2012;20(20):22344–22359.

11. Hecht E, Zajac A. Optics. Addison-Wesley Pub; 1979.

12. Chenault D, Pezzaniti L, Vaden J, Michalson J, Gurton K. Pyxis enhanced thermal imaging with division-of-focal plane polarimeter. Polarization,

Measurement, Analysis, and Remote Sensing XII, SPIE Defense & Commercial Sensing Symposia; 2016 Apr 17–24.

13. Tyo JS, Pugh EN, Engheta N. Colorimetric representations for use with polarization-difference imaging of objects in scattering media. J Opt Soc Am. A. 1999;15:367–374.

14. Ruffo GH. LIDAR? Tesla is getting rid of radars to adopt Tesla vision. Insideevs; 2021 May 26. https://insideevs.com/news/509647/tesla-vision-getting-rid-radars/.

List of Symbols, Abbreviations, and Acronyms

2-D	two-dimensional
AI	artificial intelligence
DOD	Department of Defense
DoLP	degree of linear polarization
FPA	focal-plane array
IR	infrared
LIDAR	light-detection-and-ranging
LWIR	longwave-infrared
MidIR	midwave-infrared
ML	machine learning
RADAR	radio-detection-and-ranging
SONAR	sound-navigation-and-ranging
SUV	sport utility vehicle

1 (PDF)	DEFENSE TECHNICAL INFORMATION CTR DTIC OCA
1 (PDF)	DEVCOM ARL FCDD RLD DCI TECH LIB
1 (PDF)	DEVCOM ARL FCDD RLC ES K GURTON